PCCP

Accepted Manuscript

ROYAL SOCIETY OF CHEMISTRY

www.rsc.org/pccp

THE SOLVATION STRUCTURE OF ALPRAZOLAM

Akshay Sridhar[†], Andrew J. Johnston[†], Luxmmi Varathan, Sylvia E. McLain* and Philip C. Biggin*

Department of Biochemistry, University of Oxford, South Parks Road, Oxford, OX1 3QU, United Kingdom.

[†]These authors contributed equally towards this work.

*To whom correspondence should be addressed.

Email: sylvia.mclain@bioch.ox.ac.uk

Email: philip.biggin@bioch.ox.ac.uk

Tel. +44 1865 613305

Fax. +44 1865 613238

Running Title: The Solvation Structure of Alprazolam

ABSTRACT

Alprazolam is a benzodiazepine that is commonly prescribed for the treatment of anxiety and other related disorders. Like other benzodiazepines, it is thought to exert its effect through interaction with $GABA_A$ receptors. However, it has also been described as a potent and selective protein interaction inhibitor of bromodomain and extra-terminal (BET) proteins. Indeed, the only crystal structure of alprazolam bound to a protein is a complex between alprazolam and the BRD4 bromodomain. The structure shows that the complex also involves many water interactions that mediate contacts between the drug and the protein, a scenario that exists in many drug-protein complexes. How such waters relate to solvation patterns of small molecules may improve our understanding of what dictates their appearance or absence in bridging positions within complexes and thus will be important in terms of future rational drug-design. Here, we use neutron diffraction in conjunction with molecular dynamics simulations to provide a detailed analysis of how water molecules interact with alprazolam in methanol/water mixtures. The agreement between the neutron diffraction and the molecular dynamics is extremely good. We discuss the results in the context of drug design.

INTRODUCTION

Benzodiazepines are psychoactive, small molecules that as a class of drugs are the most prescribed medications globally.[1] As the name suggests, the core chemical structure of benzodiazepines is a fusion of benzene and diazepine rings. They generally have sedative, amnesic and muscle relaxing properties and are used in the treatment of a range of clinical disorders including anxiety, insomnia and epilepsy.[2, 3] The main pharmacological effects of benzodiazepines are believed to result from their binding and modulating of the $GABA_A$ receptor.[4, 5] However, benzodiazepines have also been discovered to bind to the Bromodomain and Extra-terminal (BET)[6] and Translocator Protein (TSPO) family of proteins.[7]

Alprazolam (Xanax®) is the most used (and misused) member of the benzodiazepine family of drugs.[8] It is also postulated to be the most toxic drug in the family[9] and has a long residence time in the body.[10] In addition to the benzodiazepine targets GABA and BET, spectroscopic studies have predicted its binding to a range of important biomolecules including haemoglobin,[11] albumin[12, 13] and even DNA.[14]

Despite the extensive usage of alprazolam and its diverse binding capability, limited structural information exists on its conformation and hydration both in the bound and free states. The Protein Data Bank[15] contains only one structure of alprazolam bound to a protein (PDB ID: 3U5J; a complex with the bromodomain protein, BRD4(1)).[16]

The structure of alprazolam (8-chloro-1-methyl-6-phenyl-4H-s-triazolo(4,3-a)(1,4)benzodiazepine) along with the naming terminology used in this paper is shown in **Fig. 1**. The structure is comprised of four distinct benzene, chlorobenzene, diazepine and triazole ring structures. With a predominantly hydrophobic surface, alprazolam is sparingly soluble in water (~0.13 mM) and is predicted to interact with other hydrophobic drugs like fluoxetine.[13] However, an examination of its structure in complex with the bromdomain BRD4 reveals that it binds in a hydrated pocket.[16] Additionally, the triazole ring of alprazolam has been shown to mediate strong H-bond interactions with a range of acids.[17]

Understanding the hydrophilic/hydrophobic balance of small molecules through amphipathic solvation studies has been shown to yield valuable insights into how the

molecules function *in-vivo.*[18-22] In this work we investigate the atomistic solvation structure of alprazolam in methanol/water solution using neutron diffraction, Empirical Potential Structure Refinement (EPSR) and Molecular Dynamics (MD) simulations. Perfoming experiments in methanol/water mixtures provides a good system for analysing complex solvation environments. Despite methanol/water mixtures being miscible in the bulk phase, it has been reported that they can form segregated mico-clusters on atomic length scales.[23] These micro-clusters can accurately describe the hydro- or lipophilic preference of solute fragments and can thus provide insight into solvation effects in non-bulk scenarios (including for example, within binding pockets).[24-26] We thus compare our observations in methanol/water mixtures to the binding environment of alprazolam in BRD4. Finally we compare the conformations adopted by alprazolam in solution with that adopted in the BRD4-bound crystal structure.

METHODS

Sample Preparation

Alprazolam (CAS 28981-97-7) was purchased from Sigma Aldrich, verified by ^{1}H NMR and used without further purification. All isotopomers of methanol were dried over Mg that had been previously activated with I_2. The isotopomers were then refluxed at 330 K for 48 hours under vacuum before being cryogenically distilled onto pre-dried 3 Å molecular sieves. The purity of the methanol isotopomers was also verified though ^{1}H NMR. The alprazolam/methanol/water solutions for the neutron diffraction samples, all at a relative molar ratio of 1:125:125 (~0.14 M), were prepared by weight under an N_2 atmosphere.

Neutron Diffraction

Neutron diffraction with isotopic substitution is a well established experimental technique which can be used to determine the atomic structure of small molecules in solution.[18-22, 27, 28] Due to the coherent scattering length (b_i) of hydrogen (-3.74 fm) being different from from that of deuterium (6.67 fm) [29], this difference can be exploited to measure different diffraction patterns for the same chemical system.

Neutron diffraction patterns provide the static structure factor *F(Q)* - a measure of the structure in reciprocal space. *F(Q)* can be written as :

$$F(Q) = \sum_{\alpha,\beta \geq \alpha} (2 - \delta_{\alpha\beta}) \cdot c_\alpha c_\beta b_\alpha b_\beta [S_{\alpha\beta}(Q) - 1] \qquad (1)$$

where c_i and b_i are the relative concentration and coherent scattering length of atom *i* respectively and $\delta_{\alpha\beta}$ is the Kronecker delta function. *Q* is the scattering vector defined by $Q = 4\pi/\lambda \cdot sin(2\theta/2)$ where λ is the neutron wavelength and 2θ is the scattering angle. $S_{\alpha\beta}(Q)$ is the partial structure factor and is related to the radial distribution function (RDF) $g_{\alpha\beta}(r)$ by Fourier transformation:

$$S_{\alpha\beta}(Q) = 1 + 4\pi\rho \int r^2 \cdot [g_{\alpha\beta}(r) - 1] \cdot \frac{sin(Qr)}{Qr} dr \qquad (2)$$

where ρ is the atomic number density of the sample in atoms/Å^3.

In the present work, neutron diffraction measurements were performed at 323 K (to allow sufficient homogenous dissolution; alprazolam has limited solubility at 298 or 310K) on the SANDALS diffractometer at the ISIS Facility (STFC, UK). Six alprazolam solutions that differ only with respect to the isotopic composition of the solvent (**Table 1**) were measured in sample cells made from *Ti*/*Zr* alloy with a sample thickness and wall thickness of 1 mm. Diffraction data were collected for between 6 and 8.5 hours per sample (1200 μAhrs). Data for the empty cell, empty instrument and a vanadium standard were also collected for background subtraction and normalization. The data for samples, cells, empty instrument and vanadium were corrected for absorption, multiple scattering and inelasticity effects and subsequently converted to *F(Q)* using the GUDRUN program.[30]

Empirical Potential Structure Refinement

Empirical potential structure refinement (EPSR)[31] is a Monte Carlo-based technique where the atomic conformation of the system is constrained to fit a set of diffraction data. EPSR uses a box of molecules at the same concentration, density and temperature as the diffraction measurements. EPSR begins with a set of 'seed' or

starting potentials for each unique atom, where these potentials consist of a Lennard-Jones potential, defined by σ (the distance at which the potential is zero) and ε (the well depth) as well as appropriate atomic charges (q_e). These were obtained from Antechamber.[32] During the EPSR fitting process, these 'seed' potentials are iteratively refined until a good 'fit' to the diffraction data is obtained. The 'seed' potentials of all the alprazolam, methanol and water atoms are listed in the **SI Table 1**. The seed parameters do not majorly affect the results of the EPSR runs as the simulation is allowed to proceed until the difference between the computational and experimental structure factors *F(Q)* (or *g(r)* in real-space) is negligible. Work by Soper[33] suggested that simulations with different intermolecular potentials in fact lead to similar many body correlations, (*g(r)*), provided a good fit to the experimental data is obtained.

In the current EPSR simulation, the modelling box contained 25 Alprazolam, 3125 water and 3125 methanol molecules at a temperature of 323 K. The parameters of alprazolam and methanol were generated using AMBER[34] and ANTECHAMBER[32] and modified slightly to account for the atomic labelling in EPSR while maintaining electro-neutrality of the simulation box. The parameters for water were taken from the SPC/E[35] water model.

The individual site–site *g(r)*s (Eqn. (2)) can be extracted from the EPSR model as well as the average coordination number $\left(n_\alpha^\beta(r)\right)$,which gives the average number of β atoms around a central α atom at a distance between r_{min} and r_{max}, by integration of these *g(r)* functions *via*

$$n_\alpha^\beta(r) = 4\pi\rho c_\beta \int_{rmin}^{rmax} r^2 g_{\alpha\beta} dr \qquad (3)$$

Molecular Dynamics Simulation

MD simulations were carried out using GROMACS 5.0.2[36] at the same molecular ratios as EPSR (25 alprazolam molecules, 3125 methanol molecules, 3125 water molecules). The parameters of alprazolam and methanol initially parametrized using AMBER were converted to GROMACS format using the *acpype* script.[37] The water molecules were modelled using the SPC/E[35] model. All of the bonds and angles for the water molecules were constrained using the SHAKE[38] algorithm.

Initially, energy minimization corrected atomic overlaps up to the point where the maximum force on any atoms was below 100 kJ mol^{-1} nm^{-1}. Energy minimization was followed by a solute restrained equilibration runs of 1 ns each in the NVT and NPT ensembles. The Berendsen[39] thermostat and barostat were used to maintain temperature and pressure in the equilibration runs. Simulations were performed at the same temperature as the EPSR experiments (323 K) and the pressure was set at 1 bar.

The production runs in both simulation boxes were carried out in the NPT ensemble for 40 ns with a timestep of 2 fs. Temperature was maintained using the V-rescale thermostat while pressure was controlled using the Parinello-Rahman[40] barostat. A cut-off of 14 Å was used for the van-der-Waals interactions and long range interactions were calculated using the particle mesh Ewald (PME) algorithm.[41, 42] Coordinates were saved every 0.8 ps, resulting in 50,000 frames. Sub-sampling analysis revealed that RDF plots converged well under 1 ns of simulation, but nevertheless to remove any possibility that that initial seed values could trap the system in minima we repeated the simulations an additional four times. The RDFs in each case were identical. This apparent relaxation time for water is consistent with other studies. For example, Yang *et al*.[43] studied the effects of simulation time on the hydration of two proteins; Goose Egg-white Lysozyme and *Mycobacterium tubeculosis* pyridoxine oxidase and despite the much larger systems noted that IFST energetics (and hence by inference g(r)) converged between 1 and 2.5 ns. Thus 40 ns simulation time is more than adequate to reach convergence.

Spatial Density Analysis

The three dimensional arrangements of molecules relative to one-another was extracted from both the MD and EPSR simulations using the ANGULA[44] program. Orthogonal coordinate systems were assigned to the different fragments of alprazolam, the water molecules and to the methanol molecules (see **SI Figure 1**). Using the origins of these coordinate systems, the distributions of the nearest neighbour methanol/water molecules were plotted relative to fragments of alprazolam. The angles between the sets of axes assigned to the solute and the solvent molecules were also used to find the orientation of the solvent molecules relative to alprazolam.

Whole molecule analysis (WMA) was also performed on the EPSR simulation box using ANGULA.[22] WMA was performed for a distance range of 0–4 Å for methanol/water molecules around alprazolam, enabling the aggregate distribution to be plotted with reference to the whole molecule. In the case MD simulations, the three-dimensional arrangements of molecules were generated through Python MDAnalysis[45] scripts using the 3D Rotation Matrix algorithm.[46] The three dimensional spatial density maps (SDM)[47] were plotted using the *scipy*, *matplotlib*[48] and *mayavi*[49] libraries.

RESULTS AND DISCUSSION

To gain insight into the hydration properties of alprazolam, we first compared the calculated scattering functions, *F(Q)*, from the MD and EPSR simulations with the measured data. The comparison is summarized in **Fig. 2 (and SI Fig 2).** The EPSR fits to the *F(Q)* data are generally good with only small differences occurring at small *Q* values (**Fig. 2A**). This is largely due to the difficulty in correcting for inelastic scattering in this region of data.[50]

Methanol Interactions with Alprazolam

To understand how methanol interacts with alprazolam, we examined the radial distribution function (RDF) of the oxygen atom of methanol around each of the four ring structures of alprazolam from EPSR and MD (**Fig. 3**).

Fig. 3A-D shows the atom-averaged RDFs of the methanol O atoms around each of the four rings of alprazolam. We also examined the spatial density map (SDM) of the location of the nearest neighbour methanol from the ring centre in EPSR (**Fig. 3E-H**) and MD (**Fig. 3I-L**), where the agreement between EPSR and MD is extremely good.

The *g(r)* of methanol around the triazole ring describes two minor peaks at ~3.0 Å and ~5.5 Å (**Fig. 3A**). The first peak at ~3.0 Å is probably caused by the methanol OH group hydrogen bonding with the N5 atom as it is close to the O-H--N Hydrogen bond length.[51] The MD slightly overestimates these interactions compared with EPSR and its SDM (**Fig. 3I**) correspondingly shows a greater density when compared to EPSR (**Fig. 3E**). The second peak at ~5.5 Å is close to the observed distance for the second solvation shell. With MD simulations predicting a greater number of methanol molecules in the first shell, its prediction for the methanol density in the second shell is correspondingly lower.

The g(r)s of methanol around the chlorobenzene and diazepine rings (**Fig. 3B, C**) show no major discernible peaks. This suggests that methanol molecules are diffuse around these ring structures with no preferential residence sites. The SDMs (**Fig. 3F,G, J and K**) also support this, where the contour describing the positions of methanol is dispersed around these ring systems.

The *g(r)* of methanol around the benzene ring (**Fig. 3D**) however shows a small peak at ~5 Å. This peak is slightly more ponounced in MD simulations than in EPSR. Correspondingly in the SDMs, the contour describes a preference for methanol to reside in a position normal to the plane of the aromatic ring. Additionally, the slightly more prominent peak in MD simulations is evident in the marginally greater density of its SDM (**Fig. 3L**) compared to EPSR (**Fig. 3H**).

Water Interactions with Alprazolam

The water oxygen RDFs with the four ring systems are shown in **Fig. 4A-D**. SDMs of the location of the nearest water from the ring centre in EPSR (**Fig. 4E-H**) and MD (**Fig. 4I-L**) are also shown. While qualitatively similar, the EPSR and MD predictions diverge to a greater extent quantitively when compared to the methanol solvation

analysis (F**ig 3).** EPSR consistently predicts greater hydration across all rings of alprazolam.

Similar to the methanol solvation, the hydration of triazole shows a peak at 3 Å. This OH--N hydrogen bond is also reflected in the SDM map which displays a sharp density profile around the two N5 atoms (**Fig. 4E, I)**. However, in contrast to methanol, both EPSR and MD display no second peak and thus water resides in a diffuse manner within the second solvation shell (**see SI Fig 3**).

The *g(r)* for water around both benzene rings show no peak (**Fig. 4B, D**). Consistently, the SDM contours of water around them are diffuse with few preferential orientations (**Fig. 4 F,J H and L**). This diffuse density with little localization might be due to the triazole ring structure offering greater electrostatic H-bonding opportunities and thus reducing water-benzene interactions.

While both EPSR (**Fig. 4G**) and MD (**Fig. 4K**) predict the localization, the interaction is comparatively more directional in MD (**Fig. 4K**). The dissimilarity between the SDM and RDF could be attributed to the N2-O_w interactions being averaged out over the seven atoms in the diazepine ring.

Atomistic Preferential Solvation

To compare the interaction of methanol and water with alprazolam further we examined the RDFs for specific alprazolam atoms (see **Fig. 1**) from both EPSR and MD as summarized in **Fig. 5**. In general, it can be seen that there is excellent agreement in this analysis between the MD and EPSR and supports the SDM data presented in **Figs 3 and 4**. Specifically, the N2-O_w graph explains the localized water distribution seen around the diazepine ring. The plot exhibits a distinct peak at ~3 Å (H-bond distance). The greater localization in the MD simulations compared to the EPSR simulations is also evident with the MD plot exhibiting a larger and sharper peak (**Fig. 5D**).

To further quantify the hydrophobic/hydrophilic balance of the alprazolam motifs, the preference ratio is calculated. The preference ratio, P_{met}^{wat}, calculates the preferential interactions of an atom for water over methanol. It is defined as:

$$P_{met}^{wat} = \frac{n_x^{Ow}(r)}{n_x^{Om}(r)} \quad (4)$$

where n_x^{Ow} and n_x^{Om} are the coordination numbers of water O, (O_w) and methanol O (O_m) around atom '*x'* at radius *r*. A ratio greater than 1 indicates a preference of water while a value lesser than 1 indicates the opposite. Preference ratio calculations have previously been used to study the competitive interactions of urea with polypeptides.[52, 53] To encompass the first solvation shell, the coordination numbers of water and methanol are calculated at the first minimum of the respective atoms' RDF (**Fig. 5)**.

Table 2 lists the O_m and O_w coordination numbers of the alprazolam atoms, the *r* value at which they were calculated and their corresponding preference ratios. The coordination numbers for MD and EPSR are broadly similar with MD predicting slightly greater hydration of polar atoms than EPSR. With the limited solubility of alprazolam in water, all atoms have a preference ratio < 1, indicating a preference for methanol over water at all atomic sites. However, the solvent exposed polar N5 and N2 atoms interact the most with water and as such have the largest preference ratios. Additionally, the directionality of the water shell around N2 in **Fig. 3** is further corroborated with the adjacent C7 and CN2 atoms having markedly lower preference ratios.

Alprazolam-Alprazolam Interactions.

Interactions between alprazolam molecules tends to occur through stacking of the diazepine rings (see **SI Fig. 4**). To compare alprazolam-alprazolam interactions between MD and EPSR, we examined the inter-molecular RDF functions of a few representative atoms (data not shown). In all cases, MD predicts slightly greater alprazolam-alprazolam interactions than EPSR. These findings are in line with previous combined EPSR/MD combination studies which show a slightly greater prevalence of inter-solute interactions in MD.[54, 55] However, the alprazolam-alprazolam interactions are transient as reflected in the appearance/disappearance

of dimers and trimers compared to monomers in the system (see **SI Fig. 5**). Averaging of the hydration shell across many frames of a long simulation trajectory negates the effects of transient stacking between the molecules.

Comparing Bound and Solution States

Conformation

The conformational preferences of a compound are an important factor when considering how it may interact with other hydrophobic/hydrophilic components in a system. Thus we also examined the conformational behaviour of alprazolam. With fused chlorobenzene, diazepine and triazole rings, the benzene ring remains the most mobile in solution. The conformational analysis of the EPSR simulation carried out using ANGULA further supports this. An overlay of the different Alprazolam conformations observed over the course of the EPSR simulation is shown in **Fig. 6A**. Unlike MD, EPSR has limited bond constraints on atomic motion. Despite this, the figure highlights the limited movement of the triazole, diazepine and chlorobenzene rings. In contrast, the benzene ring is relatively mobile and is able to sample an array of conformations. In the crystallographic structure of alprazolam bound to the BRD4 bromodomain protein,[16] the benzene ring is only slightly tilted away from the plane of the molecule. In modelling studies however, Dangkoob *et al.*[13] predicted the benzene ring to adopt an orientation completely normal to the plane of the rest of the molecule. Thus we decided to analyse the conformations of alprazolam in our simulations. There is in fact only one rotatable bond (about the CN2-CB1 bond – see **Fig. 1**).

In the crystallographic structure, the benzene ring adopts a conformation slightly tilted to the molecular plane with a dihedral angle of approximately 28°. Analysing the distribution of this dihedral in MD (**Fig. 6B**) shows two major peaks at -30° and 150° which correspond to the same chemically equivalent conformation, but differs slightly from the cyrstallographic strucutre. EPSR on the other hand has two peaks at approximately -45 and 37, (**Fig. 6B**) one of which is close to the MD preferred minima and the other close to the conformer in the crystal structure complex. This

suggests that the molecular mechanics dihedral parameters are not quite optimal. We analysed this further using a quantum mechanics torsional scan, but the energy profile was identical to that produced from the molecular mechanics. Thus, other factors, not sampled, for example puckering of the diazepine ring system, may contribute to these differences. Despite these limitations, the solvation of the systems is still accurately reproduced.

The conformational analysis that EPSR can achieve here may well be useful in the context of forcefield validation and improvement. Automated parameterization methodologies for 'general' molecules such as GAFF[32] and CGenFF[56] use lookup tables of similar atoms to assign parameters for the dihedral types. However, a direct comparison to the data in the lookup tables is not always possible and this often results in 'bad' parameterization of the dihedral angles.[57] EPSR can in principle potentially be used to empirically verify the minima of dihedral angles via this approach. However, a larger and more systematic data set would be required to make substantial inroads into this problem.

Solvation

WMA of the methanol and water shells of alprazolam was also performed (**Fig. 6C**). Molecules from 5000 simulation frames were overlaid onto the crystallographic alprazolam conformation and solvent molecules within a distance range of 0-4 Å were considered. The WMA represents the most probable solvent location around all atoms of alprazolam rather than being specific to a certain site. Despite this and the marginal errors caused by the overlaying of different conformations, the WMA hydration shell closely matches the atomic preferential solvation ratios of **Table 2**. The water contour shell surrounds the N5 and N2 atoms while methanol interacts with the remaining hydrophobic motifs of the molecules. More importantly, the preferential water orientations match the locations of bridging waters from the alprazolam-BRD4 complex. The two bridging water molecules play an important role in the binding of the drug by mediating N5-Tyr97 and N2-Asn140 interactions.[58]

CONCLUSIONS

In the current investigation, we have used a combined experimental and computational approach to study the solvation of a pharmaceutically important compound - alprazolam. It is a largely hydrophobic drug with a limited solubility in water. Both MD and EPSR predicted a greater preference of alprazolam motifs to interact with methanol over water as evidenced in **Figs 3, 4** and **Table 2**. Methanol can micro-segregate in aqueous medium and offer a somewhat continuous hydrophobic surface for solvation [23]. Despite this characteristic of water/methanol solutions and the lipophilicity of alprazolam, hydrophobic effects do not completely dominate solvation.

Three solvent exposed nitrogen atoms (two N5 atoms and one N2 atom, see **Fig. 1**) form strong localized interactions with water (see Fig. 6C and Table 2). Compared to EPSR, the preferential residence sites of water around these three nitrogen atoms are more directional in MD (see Figure 4I and 4K). Previous amphipathic solvation studies of indole[19] also predict N-O_w interactions but with a broader RDF peak and thus a smaller degree of localization. The N-O_w interactions in alprazolam are highly directional and do not appear to disrupt the solvation structure around adjacent atoms.

An overlay of the O_w spatial density plot and the crystallographic conformation of alprazolam provides an interesting result. The orientation of the localized water interactions in the present solutions matches relatively accurately with the locations of bridging water molecules in the crystal structure of alprazolam bound to a bromodomain. Bridging water molecules have long been identified to play a key role in mediating protein-ligand interactions,[59-64] where they act as a 'glue' between ligand and protein[65] and can also dictate specificity.[66] Due to their importance in ligand binding and thereby drug discovery,[67-69] considerable effort has gone into predicting the location of these water molecules. Multiple empirical and knowledge-based protocols have been developed for this purpose.[70-73] However, many of these algorithms, such as Consolv[73] and WaterDock[74] for example, explicitly predict limited or no role for the ligand in determining the positions of bridging waters. The work we present here, along with previous investigations on the hydration of cocaine in solution[22], suggest this may be a significant omission for algorithms that predict the

position of bridging water sites. The cocaine study[22] also reported a correlation between the localization of water in solution and the site of crystallographic bridging waters.

At the current time, there is insufficient evidence available to further study this correlation. There are two main issues: 1) Limited solvation studies of pharmaceutically relevant ligands have been performed and 2) Waters in crystallographic structures are difficult to locate for many different reasons including high mobility, artifactual reasons due to the crystallisation conditions or poor resolution[75]. Further efforts are underway to validate this relationship and indeed to evaluate if it can be used in improved prediction of binding affinities of drugs for proteins.

Acknowledgements

The authors would like to thank the UK Engineering and Physical Sciences Research Council (EP/J002615/1) for funding and the ISIS Facility (STFC, UK) for allocation of neutron beam time. We thank Matteo Aldeghi for useful discussions.

References

1. C. Haw and J. Stubbs, J. Psychopharm., 2007, 21, 645-649.
2. J. Riss, J. Cloyd, J. Gates and S. Collins, Acta Neurol. Scand., 2008, 118, 69-86.
3. A. M. Holbrook, R. Crowther, A. Lotter, C. Cheng and D. King, Can. Med. Assoc. J., 2000, 162, 225-233.
4. F. Petty, M. H. Trivedi, M. Fulton and A. John Rush, Biol. Psychiatry, 1995, 38, 578-591.
5. W. Hunkeler, H. Mohler, L. Pieri, P. Polc, E. P. Bonetti, R. Cumin, R. Schaffner and W. Haefely, Nature, 1981, 290, 514-516.
6. P. Filippakopoulos, J. Qi, S. Picaud, Y. Shen, W. B. Smith, O. Fedorov, E. M. Morse, T. Keates, T. T. Hickman, I. Felletar, M. Philpott, S. Munro, M. R. McKeown, Y. Wang, A. L. Christie, N. West, M. J. Cameron, B. Schwartz, T. D. Heightman, N. La Thangue, C. A. French, O. Wiest, A. L. Kung, S. Knapp and J. E. Bradner, Nature, 2010, 468, 1067-1073.

7. T. Sabrina, P. Isabella and S. Federico Da, Curr. Top. Med. Chem., 2011, 11, 860-886.
8. N. A. Shah, M. A. Abate, M. J. Smith, J. A. Kaplan, J. C. Kraner and D. J. Clay, Am. J. Addict., 2012, 21, S27-S34.
9. G. K. Isbister, L. O'Regan, D. Sibbritt and I. M. Whyte, Br. J. Clin. Pharmacol., 2004, 58, 88-95.
10. V. D. Schmith, B. Piraino, R. B. Smith and P. D. Kroboth, J. Clin. Pharm., 1991, 31, 571-579.
11. S. Maitra, B. Saha, C. R. Santra, A. Mukherjee, S. Goswami, P. K. Chanda and P. Karmakar, Int. J. Biol. Macromol., 2007, 41, 23-29.
12. M. Sarkar, S. S. Paul and K. K. Mukherjea, Journal of Luminescence, 2013, 142, 220-230.
13. F. Dangkoob, M. R. Housaindokht, A. Asoodeh, O. Rajabi, Z. Rouhbakhsh Zaeri and A. Verdian Doghaei, Spectrochim. Acta A Mol. Biomol. Spectrosc., 2015, 137, 1106-1119.
14. B. Saha, A. Mukherjee, C. R. Santra, A. Chattopadhyay, A. N. Ghosh, U. Choudhuri and P. Karmakar, J. Biomol. Struct. Dyn., 2009, 26, 421-429.
15. H. Berman, K. Henrick, H. Nakamura and J. L. Markley, Nucleic Acids Res, 2007, 35, D301-D303.
16. P. Filippakopoulos, S. Picaud, O. Fedorov, M. Keller, M. Wrobel, O. Morgenstern, F. Bracher and S. Knapp, Bioorg. Med. Chem., 2012, 20, 1878-1886.
17. S. Varughese, Y. Azim and G. R. Desiraju, J Pharm Sci., 2010, 99, 3743-3753.
18. R. J. Gillams, J. V. Busto, S. Busch, F. M. Goñi, C. D. Lorenz and S. E. McLain, J. Phys. Chem. B, 2015, 119, 128-139.
19. A. J. Johnston, Y. Zhang, S. Busch, L. C. Pardo, S. Imberti and S. E. McLain, J. Phys. Chem. B., 2015, 119, 5979-5987.
20. N. H. Rhys, A. K. Soper and L. Dougan, J. Phys. Chem. B, 2015, 119, 15644-15651.
21. E. Pluhařová, H. E. Fischer, P. E. Mason and P. Jungwirth, Mol. Phys., 2014, 112, 1230-1240.
22. A. J. Johnston, S. Busch, L. C. Pardo, S. K. Callear, P. C. Biggin and S. E. McLain, Phys. Chem. Chem. Phys., 2016, 18, 991-999.
23. S. Dixit, J. Crain, W. C. K. Poon, J. L. Finney and A. K. Soper, Nature, 2002, 416, 829-832.
24. A. Vishnyakov and A. V. Neimark, J. Phys. Chem. B., 2001, 105, 7830-7834.
25. F. M. Ho and S. Styring, Biochim. Biophys. Acta, 2008, 1777, 140-153.
26. L. Dougan, S. P. Bates, R. Hargreaves, J. P. Fox, J. Crain, J. L. Finney, V. Reat and A. K. Soper, J. Chem. Phys., 2004, 121, 6456-6462.
27. S. K. Callear, A. Johnston, S. E. McLain and S. Imberti, J. Chem. Phys., 2015, 142, 014502.
28. J. J. Shephard, A. K. Soper, S. K. Callear, S. Imberti, J. S. O. Evans and C. G. Salzmann, Chem. Comms., 2015, 51, 4770-4773.
29. V. V. F. Sears, Neutron News, 1992, 3, 26-37.
30. A. K. Soper, GudrunN and GudrunX: Programs for correcting raw neutron and X-ray diffraction data to differential scattering cross section, (2011) Rutherford Appleton Laboratory, STFC, UK.
31. A. K. Soper, Mol. Simul., 2012, 38, 1171-1185.

32. J. Wang, W. Wang, P. A. Kollman and D. A. Case, J. Mol. Graph. Mod., 2006, 25, 247-260.
33. A. K. Soper, Mol. Phys., 2001, 99, 1503-1516.
34. D. A. Case, T. E. Cheatham, T. O. M. Darden, H. Gohlke, R. A. Y. Luo, K. M. Merz, A. Onufriev, C. Simmerling, B. Wang and R. J. Woods, J. Comp. Chem., 2005, 26, 1668-1688.
35. H. J. C. Berendsen, J. R. Grigera and T. P. Straatsma, J. Phys. Chem., 1987, 91, 6269-6271.
36. D. van der Spoel, E. Lindahl, B. Hess, G. Groenhof, A. E. Mark and H. J. C. Berendsen, J. Comput. Chem., 2005, 26, 1701-1718.
37. A. Sousa da Silva and W. Vranken, BMC Res. Notes, 2012, 5, 367.
38. J. P. Ryckaert, G. Ciccotti and H. J. C. Berendsen, J. Comput. Phys., 1977, 23, 327.
39. H. J. C. Berendsen, J. P. M. Postma, W. F. van Gunsteren, A. DiNola and J. R. Haak, J. Chem. Phys., 1984, 81, 3684-3690.
40. M. Parinello and A. Rahman, J. Appl. Phys., 1981, 52, 7182-7190.
41. U. Essman, L. Perera, M. L. Berkowitz, T. Darden, H. Lee and L. G. Pedersen, J. Chem. Phys., 1995, 103, 8577-8593.
42. T. Darden, D. York and L. Pedersen, J. Chem. Phys., 1993, 98, 10089-10092.
43. Y. Yang, B. Hu and M. A. Lill, J. Chem. Inf. Model., 2014, 54, 2987-2995.
44. L. C. Pardo, M. Rovira-Esteva, J. L. Tamarit, N. Veglio, F. J. Bermejo and G. J. Cuello, Metastable Systems under Pressure, Springer Netherlands, 2010.
45. N. Michaud-Agrawal, E. J. Denning, T. Woolf and O. Beckstein, J. Comput. Chem., 2011, 32, 2319-2327.
46. P. Liu, D. K. Agrafiotis and D. L. Theobald, J. Comp. Chem., 2010, 31, 1561-1563.
47. S. Busch, C. D. Lorenz, J. Taylor, L. C. Pardo and S. E. McLain, J. Phys. Chem. B, 2014, 118, 14267-14277.
48. J. D. Hunter, Comput. Sci. Eng., 2007, 9., 90-95.
49. P. Ramachandran and G. Varoquaux, IEEE Comput. Sci. Eng., 2011, 13, 40-51.
50. A. K. Soper, Mol. Phys., 2009, 107, 1667-1684.
51. G. Rossato, B. Ernst, A. Vedani and M. Smiesko, J Chem Inf Model, 51, 1867-1881.
52. M. C. Stumpe and H. Grubmüller, J. Am. Chem. Soc., 2007, 129, 16126-16131.
53. N. Steinke, R. J. Gillams, L. C. Pardo, C. D. Lorenz and S. E. McLain, Phys. Chem. Chem. Phys., 2016, 18, 3862-3870.
54. L. Tavagnacco, J. W. Brady, F. Bruni, S. Callear, M. A. Ricci, M. L. Saboungi and A. Cesàro, J. Phys. Chem. B, 2015, 119, 13294-13301.
55. F. Foglia, M. J. Lawrence, C. D. Lorenz and S. E. McLain, J. Chem. Phys., 2010, 133, 145103.
56. V. Zoete, M. Cuendet, A. Grosdidier and O. Michielin, J. Comput. Chem., 2011, 32, 2359-2368.
57. L. Huang and B. Roux, J. Chem. Theory Comput., 2013, 9, 3543-3556.
58. M. Aldeghi, A. Heifetz, M. J. Bodkin, S. Knapp and P. C. Biggin, Chem. Sci., 2016, 7, 207-218.
59. J. R. H. Tame, S. H. Sleigh, A. J. Wilkinson and J. E. Ladbury, Nat. Struct. Biol., 1998, 998-1001.
60. R. U. Lemieux, Acc. Chem. Res., 1996, 29, 373-380.

61. T. Okada, Y. Fujiyoshi, M. Silow, J. Navarro, E. M. Landau and Y. Shichida, Proc. Natl. Acad. Sci. USA, 2002, 99, 5982-5987.
62. F. A. Quiocho, D. K. Wilson and N. K. Vyas, Nature, 1989, 340, 404-407.
63. Ni, C. A. Sotriffer and J. A. McCammon, J. Med. Chem., 2001, 44, 3043-3047.
64. J. Vogt, R. Perozzo, A. Pautsch, A. Prota, P. Schelling, B. Pilger, G. Folkers, L. Scapozza and G. E. Schulz, Proteins: Struct. Func. Bioinf., 2000, 41, 545-553.
65. S. Amiri, M. S. P. Sansom and P. C. Biggin, Protein Eng. Des. Sel., 2007, 20, 353-359.
66. Y. Lu, R. Wang, C.-Y. Yang and S. Wang, J. Chem. Inf. Model., 2007, 47, 668-675.
67. A. T. García-Sosa, J. Chem. Inf. Model., 2013, 53, 1388-1405.
68. R. Kadirvelraj, B. L. Foley, J. D. Dyekjaer and R. J. Woods, J. Am. Chem. Soc., 2008, 130, 16933-16942.
69. D. G. LLoyd, A. T. Garcia-Sosa, I. L. Alberts, N. P. Todorov and R. L. Mancera, J. Comp. Aided Mol. Des., 2004, 18, 89-100.
70. E. P. Raman and A. D. MacKerell, J. Chem. Phys., 2013, 139, 055105.
71. C. N. Nguyen, T. Kurtzman Young and M. K. Gilson, J. Chem. Phys., 2012, 137, 044101.
72. B. Hu and M. A. Lill, J. Cheminform., 2014, 6, 1-14.
73. A. T. Garcia-Sosa, R. L. Mancera and P. M. Dean, J. Mol. Model., 2003, 9, 172-182.
74. G. A. Ross, G. M. Morris and P. C. Biggin, PLoS ONE, 2012, 7, e32036.
75. O. Carugo and D. Bordo, Acta Crystallogr. Sect. D Biol. Crystallogr., 1999, 55, 479-483.

Tables

Table 1. Summary of sample composition.

Sample Number	Sample Name	Methanol	Water
1	alprazolam/CH_3OH/H_2O	CH_3OH	H_2O
2	alprazolam/CHD_3OH/H_2O	$CH_{1.5}D_{1.5}OH$	H_2O
3	alprazolam/CH_3OD/D_2O	CH_3OD	D_2O
4	alprazolam/CD_3OD/D_2O	CD_3OD	D_2O
5	alprazolam/CHD_3OD/D_2O	$CH_{1.5}$ $D_{1.5}OD$	D_2O
6	alprazolam/CD_3OHD/HDO	$CD_3OD_{0.5}H_{0.5}$	HDO

Table 2. Summary of properties for key atoms.

Atom	*r (Å)*	n^{Ow} MD -- EPSR	n^{Om} MD -- EPSR	P_{met}^{wat} MD --EPSR
N5	3.84	0.86 -- 0.88	1.01 -- 0.95	0.847 -- 0.926
C7	4.38	1.04 -- 1.28	1.74 -- 1.81	0.598 -- 0.707
N2	3.44	0.25 -- 0.24	0.29 -- 0.16	0.861 -- 1.500
CN2	4.42	0.43 -- 0.48	0.73 -- 0.62	0.578 -- 0.774
CL1	4.68	1.36 --2.41	2.90 -- 2.68	0.467 -- 0.899
CB	4.24	0.74 -- 0.90	1.30 -- 1.06	0.565 -- 0.849

Water and methanol co-ordination numbers of key alprazolam atoms from MD and EPSR. Also included is the position *r* at which the values were calculated which correspond to the first minima of the RDF plots in Fig. 5.

FIGURE CAPTIONS

Figure 1. The molecular structure of alprazolam with atom labelling used in this work.

Figure 2. Plot showing the comparison of the measured F(Q) (coloured lines) with the EPSR (**A**) and MD (**B**) fits (black lines) to the data for different deuterated compositions, shifted in the Y axis for clarity by the amount indicated in each case. The differences between the data are shown as grey lines and shift by -0.5 for clarity.

Figure 3. (A-D) RDFs of the oxygen atom of methanol around each of the four ring structures of alprazolam from EPSR and MD at 323 K. **(E-H)** Spatial density maps (SDM)s of the nearest methanol oxygen around the corresponding ring structures from EPSR. (**I-L**) SDMs of the nearest methanol oxygen around the corresponding ring structures from MD. The locations of the nearest neighbour for the SDMs are calculated from the ring center and the isocontour surfaces enclose the densest 30% of sites. The scale bar shows the local number density of neighbours in $Å^{-3}$.

Figure 4. (A-D) RDFs of the oxygen atom of water around each of the four ring structures of alprazolam from EPSR and MD at 323 K. (**E-H**) SDMs of the nearest water oxygen around the corresponding ring structures from EPSR. (**I-L**) SDMs of the nearest water oxygen around the corresponding ring structures from MD. As for Fig. 3, the locations of the nearest neighbour water oxygen are calculated from the ring center and the isocontour surfaces enclose the densest 30% of sites. The scale bar shows the local number density of neighbours in $Å^{-3}$.

Figure 5. RDFs from EPSR (blue) and MD (red) of methanol and water oxygen around key atoms of alprazolam. The RDFs for water (dashed lines) are shifted by 1.5 units for clarity. The minimum points of these graphs are used for the preference ratio calculations in **Table 2**.

Figure 6. (A) Overlay of four different alprazolam molecules obtained from WMA of EPSR to demonstrate the conformations adopted by the aromatic ring. **(B)** Distribution of dihedral angles subtended by the rotation of the CN2-CB1 bond in the MD simulations. **(C)** WMA of MD simulations with the green and grey solvent clouds showing the probable locations of the top 35 % of water and methanol molecules respectively. The crystallographic bridging water molecule sites (PDB ID: 3U5J) are shown as red spheres.

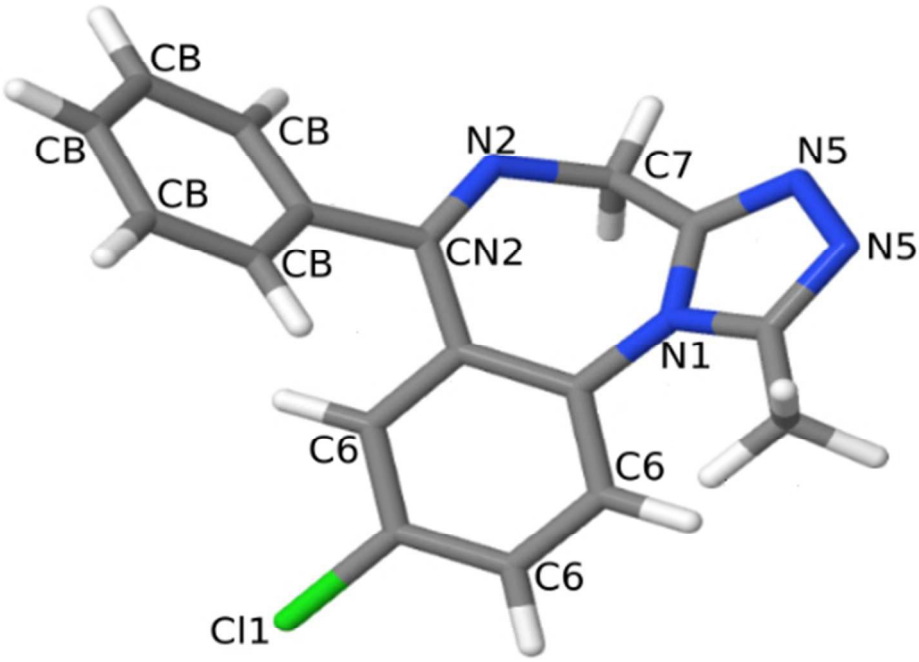

Figure 1. The molecular structure of alprazolam with atom labelling used in this work.
Fig. 1
147x111mm (96 x 96 DPI)

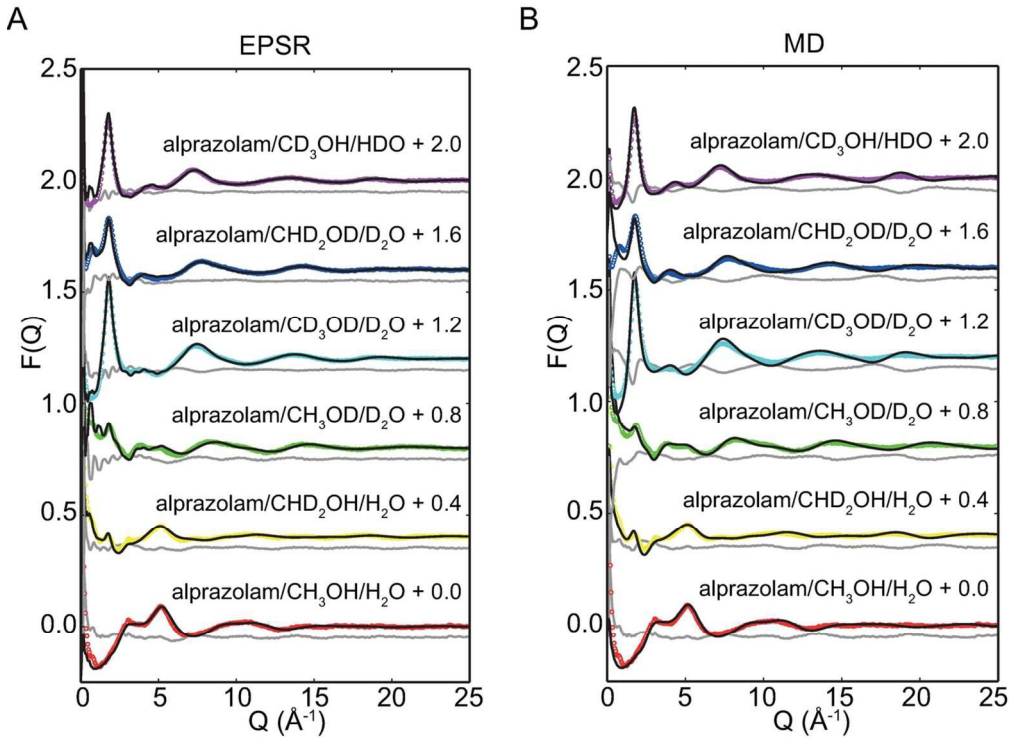

Figure 2. Plot showing the comparison of the measured F(Q) (coloured lines) with the EPSR (A) and MD (B) fits (black lines) to the data for different deuterated compositions, shifted in the Y axis for clarity by the amount indicated in each case. The differences between the data are shown as grey lines and shift by -0.5 for clarity.

Fig. 2
116x85mm (300 x 300 DPI)

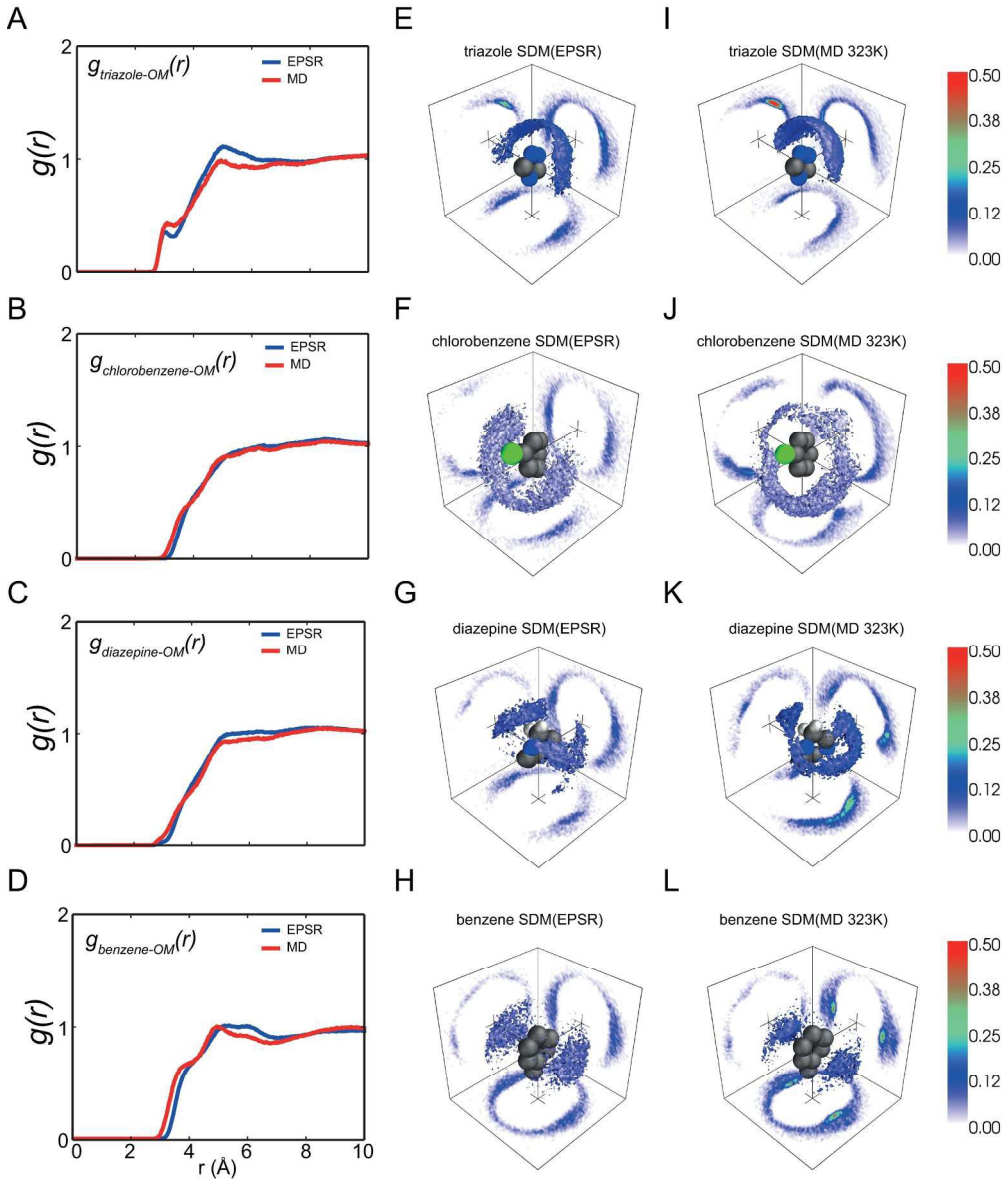

Figure 3. (A-D) RDFs of the oxygen atom of methanol around each of the four ring structures of alprazolam from EPSR and MD at 323 K. (E-H) Spatial density maps (SDM)s of the nearest methanol oxygen around the corresponding ring structures from EPSR. (I-L) SDMs of the nearest methanol oxygen around the corresponding ring structures from MD. The locations of the nearest neighbour for the SDMs are calculated from the ring center and the isocontour surfaces enclose the densest 30% of sites. The scale bar shows the local number density of neighbours in $Å^{-3}$

Fig. 3
220x259mm (300 x 300 DPI)

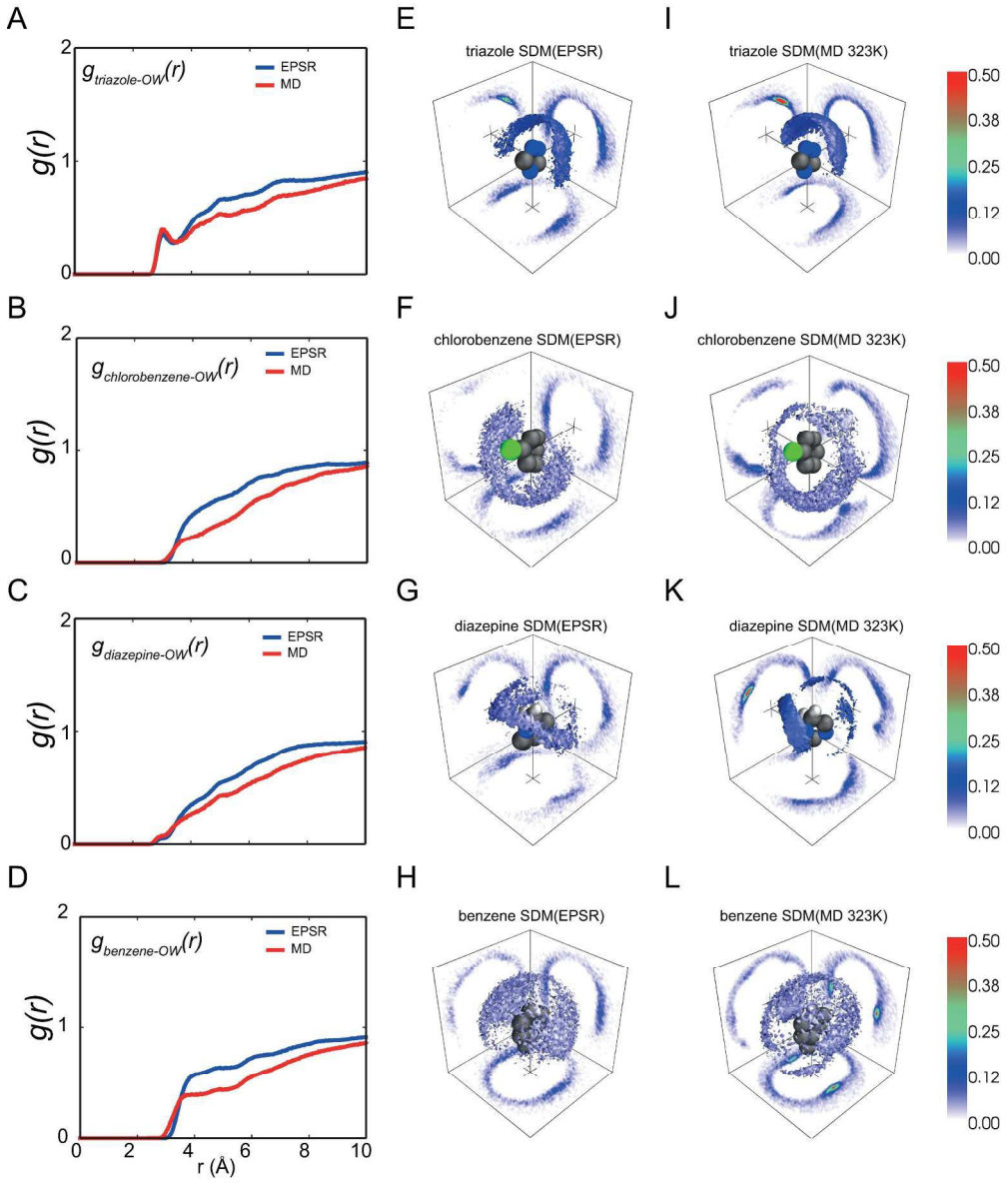

Figure 4. (A-D) RDFs of the oxygen atom of water around each of the four ring structures of alprazolam from EPSR and MD at 323 K. (E-H) SDMs of the nearest water oxygen around the corresponding ring structures from EPSR. (I-L) SDMs of the nearest water oxygen around the corresponding ring structures from MD. As for Fig. 3, the locations of the nearest neighbour water oxygen are calculated from the ring center and the isocontour surfaces enclose the densest 30% of sites. The scale bar shows the local number density of neighbours in $Å^{-3}$.

Fig. 4
221x259mm (300 x 300 DPI)

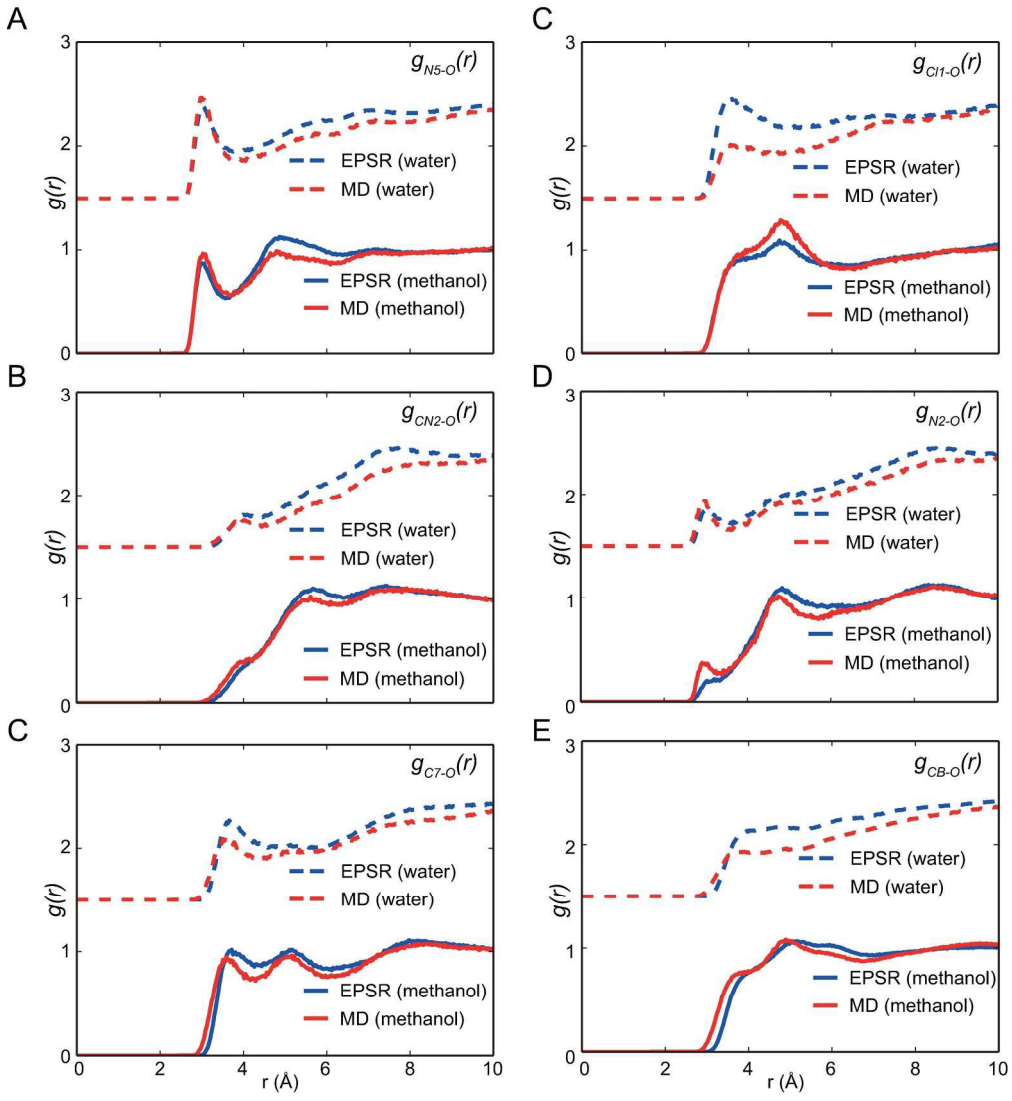

Figure 5. RDFs from EPSR (blue) and MD (red) of methanol and water oxygen around key atoms of alprazolam. The RDFs for water (dashed lines) are shifted by 1.5 units for clarity. The minimum points of these graphs are used for the preference ratio calculations in Table 2.

Fig. 5

204x222mm (300 x 300 DPI)

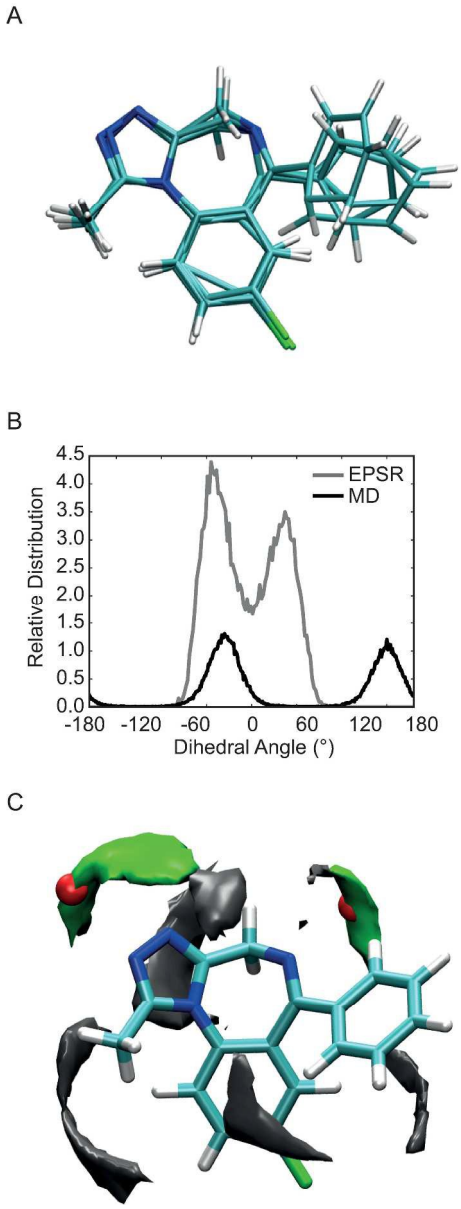

Figure 6. (A) Overlay of four different alprazolam molecules obtained from WMA of EPSR to demonstrate the conformations adopted by the aromatic ring. (B) Distribution of dihedral angles subtended by the rotation of the CN2-CB1 bond in the MD simulations. (C) WMA of MD simulations with the green and grey solvent clouds showing the probable locations of the top 35 % of water and methanol molecules respectively. The crystallographic bridging water molecule sites (PDB ID: 3U5J) are shown as red spheres.
Fig. 6
247x645mm (300 x 300 DPI)